Droplet vaporization at critical conditions: Long-time convective-diffusive profiles along the critical isobar

Manuel Arias-Zugasti,[1] Pedro L. García-Ybarra,[2] and Jose L. Castillo[1]
[1]*Departamento de Física Matemática y Fluidos, UNED, Apartado 60141, 28080 Madrid, Spain*
[2]*Departamento de Combustibles Fósiles, CIEMAT, Avenida Complutense 22, 28040 Madrid, Spain*
(Received 30 July 1998; revised manuscript received 9 April 1999)

The heating of a cold fluid package introduced, at critical conditions, in a hotter environment of the same fluid at the critical pressure is analyzed. Critical anomalies of the fluid transport properties as well as an arbitrary equation of state are taken into account. In unconfined microgravity conditions and for times much longer than the characteristic acoustic time, the heat transfer becomes a convective-diffusive isobaric transient process. An asymptotic theory valid in the limit of very small ratio between the fluid densities in the hot and cold regions is developed. The divergency of the thermal conductivity κ at the critical temperature controls the heat transfer to the cold region. In the present model it is shown that there exists a well defined border, denoted by $R(t)$, delimiting two distinguishable regions. The outer region extends from the far field down to $R(t)$ where the critical temperature T_c is reached. There, the temperature gradient vanishes due to the divergency of κ. Thus, heat does not penetrate in the inner cold region where the temperature remains equal to T_c. The heating of the initially cold fluid package takes place by the recession of the border $R(t)$. The model predicts a temperature profile in the outer region which is quasisteady in a reference system receding with $R(t)$. It is shown that $R^2(t)$ decreases linearly with time. The recession velocity and thus the vaporization time are obtained as a function of the geometry and of the far-field conditions. Furthermore, the restrictions imposed by the long-time isobaric hypothesis are analyzed. [S1063-651X(99)01009-0]

PACS number(s): 44.10.+i, 44.25.+f, 64.60.Ht

I. INTRODUCTION

The heating of an initially cold package of fluid at the critical point (CP) suddenly introduced in a much larger and hotter environment of the same fluid at critical pressure is analyzed. Buoyancy effects are not considered. Classical theories for droplet vaporization under subcritical conditions predict that the square of the droplet diameter decreases linearly with time (the so-called d^2 law). The proportionality constant provides the vaporization rate which depends on the fluid thermodynamic properties and diverges when the latent heat of vaporization vanishes. Therefore, a vanishing vaporization time is predicted for critical fluid conditions. Thus, these classical theories do not properly account for the actual behavior at and near the fluid critical pressure. The heating of the critical fluid package is analyzed in this paper with a full account of the critical behavior of the thermodynamic fluid properties at the critical point. In this work, the usual quasisteady (QS) approach (in a moving reference system) for the temperature distribution in the hot fluid region is used. The model leads again to a d^2 law but now with a nondiverging vaporization rate.

Let us consider the unsteady convection-diffusion heat transfer problem of two adjacent portions of the same fluid at different initial temperatures, such that the cold fluid portion is at the vapor-liquid CP. An enhanced heating occurs due to the piston effect if the heat transfer takes place at constant volume, as a consequence of the critical divergency of the thermal expansion coefficient. However, we will restrict ourselves to the case of an unconfined environment when the characteristic heating time is much longer than the acoustic time, as happens in many practical situations. Here, the pressure will remain almost constant and equal to the initial critical pressure P_c. Under these conditions, the temperature may attain a quasistationary profile that recedes with a given velocity. This velocity has to be obtained as part of the solution. In the present paper, the long-time isobaric evolution of the initial temperature discontinuity is outlined for various geometries, and fully solved for the spherical symmetry case which is the case of interest in droplet vaporization. It is shown that, due to the critical divergency of the thermal conductivity κ, the slope of the quasisteady temperature profile, attained for long times, must vanish at the locus where the critical temperature T_c is reached. This behavior of the temperature profile matches continuously with the theoretically predicted isobaric QS profiles found in the subcritical case, when the pressure is raised up to the critical value and the vaporization latent heat vanishes.

The following temperature discontinuity is considered as initial condition:

$$T=T_c \text{ for } r<R_{\text{in}} \quad \text{and} \quad T=T_\infty \text{ for } r>R_{\text{in}}, \tag{1}$$

where r is the relevant spatial coordinate and R stands for the location of the border separating the cold fluid at the CP from the heated fluid. The subscript c stands for critical conditions, the subscript ∞ refers to the initial conditions in the hot region, and subscript ''in'' denotes initial values.

The pressure is considered to remain equal to the critical pressure $P=P_c$. Then, the velocity field and temperature distribution are governed by the continuity equation and the energy equation. The moment conservation equation can be used to determine the validity limits of the isobaric hypothesis.

This paper is organized as follows. A brief review of present droplet vaporization theories in subcritical as well as supercritical fluid conditions is outlined in Sec. II. As the classical analyses fail down near the fluid critical conditions, a new model is presented in this paper. For critical conditions, the position where T reaches the critical value T_c from the hotter side defines a characteristic locus which plays the role of the gas-liquid interface in subcritical conditions. The properties of this locus are presented in Sec. III. The quasisteady temperature profiles are solved in Sec. IV where the d^2 law and the critical vaporization rate are obtained. Also in Sec. IV the restrictions imposed by the model are discussed. Section V applies the results to a van der Waals fluid at critical conditions. The discussion of results is provided in Sec. VI.

II. DROPLET VAPORIZATION THEORIES

The problem of droplet vaporization/combustion in unconfined media is usually treated as isobaric (i.e., the velocity induced by the Stefan flow assumed to be much smaller than the sound speed), spherically symmetrical (neglecting buoyancy effects), and diffusion controlled. See [1–5] for a review.

In subcritical conditions the classical theory predicts that there exists an initial transient period for the whole droplet to reach the vaporization wet-bulb temperature. The amount of fluid vaporized during this transient phase is often negligible. Afterwards the vaporization proceeds in a QS manner such that the squared diameter of the droplet decreases linearly with time (d^2 law). Then, the vaporization rate defined as

$$K'_{\mathrm{vap}} \equiv -\frac{dR^2}{dt} = \frac{R_{\mathrm{in}}^2}{t_{\mathrm{vap}}} \tag{2}$$

is constant. t_{vap} is the characteristic droplet vaporization time and R is the instantaneous droplet radius.

Depending on the initial droplet temperature, the transient heating period in the liquid phase may last for an appreciable fraction of the droplet lifetime. The transient period in the gas phase close to the droplet (induced by the initial temperature discontinuity) has been found to be negligible. The validity of this QS theory is explained as a consequence of the very small density ratio between the gas density and the liquid density

$$\varepsilon \equiv \frac{\rho_\infty}{\rho_{\mathrm{in}}} \ll 1 \tag{3}$$

that causes in the gas an intense Stefan flow and a very large characteristic Strouhal number. The unsteady corrections to the QS theory are, as explained by [6], due to the influence of the unsteady far-field region, at distances of order $R_{\mathrm{in}}/\sqrt{\varepsilon}$, where convection is negligible as compared to diffusion. These unsteady corrections of the QS model are of order $O(\varepsilon^{1/2})$.

In these subcritical conditions when variable properties are taken into account, the d^2 law and the vaporization constant predicted by the classical theory are in good agreement with experiment [2], resulting in

$$K'_{\mathrm{vap}} \propto \ln\left(1 + \frac{\langle c_P \rangle (T_\infty - T_{\mathrm{in}})}{L}\right), \tag{4}$$

where $\langle c_P \rangle$ is an averaged value of the specific heat at constant pressure (and this average behaves regularly at the critical point) and L is the specific latent heat of vaporization (which vanishes when the critical temperature is approached).

Therefore, Eq. (4) shows that the classical theory predicts a divergency of the vaporization rate, as the pressure approaches the fluid critical pressure where L vanishes. Thus, a fluid at critical pressure seems to vaporize instantaneously due to the vanishing of L. That would mean that as soon as a pocket of cold fluid is introduced in a much hotter environment filled with the same fluid at the critical pressure, there is no distinction between the two initial regions and a continuous phase represents the evolution of the heat transfer problem. However, experiments [7–11] have shown that even for ambient pressures equal to the fluid critical pressure or larger, there still exists a characteristic time of heat conduction. During this time a well defined cold region remains distinguishable from the heated fluid side. This behavior cannot be obtained from the classical theory. The present paper tries to solve the discrepancy between the classical theory and the experimental findings.

Spalding [12], in order to compute droplet combustion times, considered that under critical or supercritical conditions the droplet could be considered as an instantaneous point source (PS) of gas (PS theory). In this PS theory the density is taken as constant in the gas phase and, consequently, convective transport is neglected, but unsteady conduction of heat is taken into account. Rosner [13] generalized the former PS theory to account for the finite size of the supercritical pocket of gas. Like the PS theory, the distributed source theory neglected the convective heat transfer in the gas surrounding the droplet. Sánchez-Tarifa *et al.* [14] analyzed the vaporization time of a supercritical droplet in a gas phase considered as an ideal gas with variable thermal conductivity and constant specific heat. In their analysis the space was divided into three distinct regions, the outer QS region, the inner receding transition region, and the cold droplet. Each region was solved separately and the recession rate of the transition region was obtained by the matching between the temperature profiles in the different regions. They also found a d^2 law for the vaporization dynamics applicable when the heating takes place at supercritical pressures. The present work is based on the analysis by Sánchez-Tarifa *et al.* [14], but includes the critical behavior of the fluid transport coefficients at the critical temperature. In our analysis, the transition region indicated by Sánchez-Tarifa *et al.* becomes engulfed by the outer region and only two distinguishable fluid regions should be accounted for.

The problem of droplet vaporization in contact with a multicomponent gas has been studied by several authors. Rosner and Chang [15] considered the vaporization and combustion problem of a monocomponent droplet in near critical conditions in contact with a multicomponent gas. In their model the properties in both phases, including the gas density, were substituted by appropriate averaged values and the actual behavior of the latent heat was taken into account. They obtained the stationary wet-bulb temperature for the

liquid phase in contact with a multicomponent gas as a result of the balance between the heat transferred to the droplet by conduction and that needed for the vaporization to take place. As the pressure is raised the stationary wet-bulb temperature tends to the critical value along the coexistence curve, reaching it when the pressure is about three times the critical pressure of the fuel. For pressures larger than nearly three times the fuel critical pressure, a subcritical stationary temperature for the dense phase is never achieved. The model concludes that in these cases the vaporization will be completely unsteady. For smaller pressures the droplet will attain a subcritical stationary wet-bulb temperature even with pressures greater than the critical pressure. Haldenwang *et al.* [16] considered the problem of a liquid oxygen droplet vaporizing in contact with a hydrogen atmosphere. The thermodynamic model considered in the numerical analysis was based on a mixture equation of state obtained by means of the classical mixing rules applied to the Redlich-Kwong-Soave cubic equation of state (EOS) of the pure component. The classical mixing rules were also considered in order to approximate the specific heat of the mixture. The transport properties considered were based in empirical correlations supplemented with mixing rules in the case of the thermal conductivity. In the thermodynamic model of the mixture the singular critical behavior of the pure component thermodynamic properties was not taken into account. The study focused on the transition from subcritical to supercritical vaporization regime depending on ambient pressure and temperature. The results of the analysis showed that, as a consequence of mixture properties, subcritical vaporization regimes can be obtained even for chamber pressures much larger than the oxygen critical pressure. For larger chamber pressures the transient supercritical vaporization regime is encountered. The minimum droplet vaporization time was found to correspond to the pressure and temperature conditions where the transition between both regimes occurred.

III. THE FLUID AT CRITICAL CONDITIONS

When the vaporization takes place under subcritical conditions, there is a well defined physical interface separating the cooler and denser (liquid) phase from the hotter and lighter (gas) phase. However, the concepts of latent heat and surface tension lose their meaning beyond the critical pressure where both vanish. Thus, for pressures larger than or equal to the fluid critical pressure such an interface cannot be properly defined. However, in the present section it is shown that at the critical pressure, the locus where the critical temperature is reached (and where several fluid transport coefficients diverge) plays a role quite similar to the interface in subcritical conditions.

A. The divergencies at critical pressure

The shape of the critical isotherm, the behavior of the order parameter (the fluid density ρ), and the correlation length ξ, near the CP, are given by the well known critical laws [17,18]

$$P-P_c \propto \left(\frac{\rho-\rho_c}{\rho_c}\right)^{\delta} \text{ at } T=T_c,$$

$$\rho-\rho_c \propto \left(\frac{T-T_c}{T_c}\right)^{\beta} \text{ along the coexistence line,}$$
$$\xi \propto \left|\frac{T-T_c}{T_c}\right|^{-\nu} \text{ at } \rho=\rho_c, \tag{5}$$

where β, δ, and ν are critical exponents.

Moreover, the Einstein-Kawasaki formula [19] provides the behavior of the thermal diffusivity χ near the CP,

$$\chi=\frac{\kappa}{\rho c_P}\simeq\frac{k_B T_c}{6\pi\mu\xi}, \tag{6}$$

where κ is the thermal conductivity, c_P is the mass specific heat at constant pressure, k_B is the Boltzmann constant, and μ is the (nondiverging) fluid viscosity.

Making use of the exponent renormalization rule for the power laws along different paths [20], when one approaches the critical temperature along the critical isobar, the order parameter, the mass specific heat at constant pressure, and the thermal conductivity behave as

$$\rho-\rho_c \simeq -\rho_0\left(\frac{T-T_c}{T_c}\right)^{1/\delta} \text{ at } P=P_c,$$

$$c_P \simeq c_0\left|\frac{T-T_c}{T_c}\right|^{-\gamma/\beta\delta} \text{ at } P=P_c, \tag{7}$$

$$\kappa \simeq \rho_c\chi_0 c_0\left|\frac{T-T_c}{T_c}\right|^{-(\gamma-\nu)/\beta\delta} \text{ at } P=P_c,$$

where subscript 0 denotes the dimensional power law amplitudes along the critical isobar.

The values of the critical exponents [20] and all the critical exponent combinations of interest here are given in Table I, where the first column corresponds to the *mean field theory* and the second column to the most accurate *renormalization group* value.

TABLE I. Critical exponents and critical exponent combinations.

Critical exponent	Mean field theory	Renormalization group
α	0	0.110 ± 0.003
β	1/2	0.326 ± 0.002
γ	1	1.239 ± 0.002
δ	3	4.80 ± 0.02
ν	1/2	0.630 ± 0.001
η	0	0.031 ± 0.004
$1/\delta$	1/3	0.208 ± 0.001
$\frac{\gamma}{\beta\delta}$	2/3	0.792 ± 0.009
$\frac{\nu}{\beta\delta}$	1/3	0.403 ± 0.012
$\frac{\gamma-\nu}{\beta\delta}$	1/3	0.389 ± 0.004
$1-\frac{\nu}{\beta\delta}$	2/3	0.597 ± 0.012

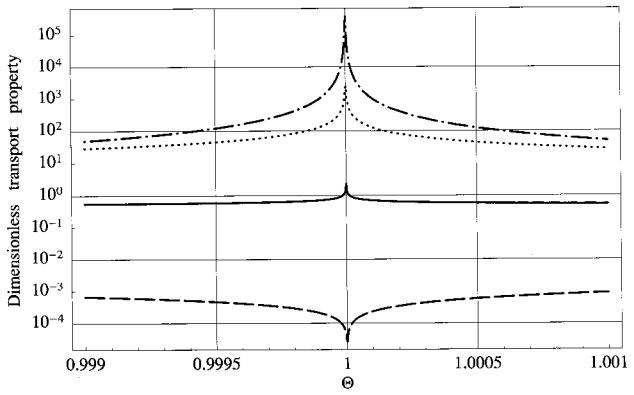

FIG. 1. Log-linear plot of $\Lambda \equiv \kappa/\kappa_\infty$ (solid line), $C \equiv c_P/c_{P_\infty}$ (dotted line), $\Lambda/\varrho C \equiv \chi/\chi_\infty$ (dashed line), and $\Lambda_\Theta \equiv |\partial\Lambda/\partial\Theta|$ (dot-dashed line) versus the reduced temperature $\Theta \equiv T/T_c$ for a van der Waals fluid in the critical region with $P=P_c$, $T_\infty = 9.3T_c$, $c_v = \frac{3}{2}\mathcal{R}_m$, and κ given by Eqs. (58) and (60)–(62) with $\kappa_0 = 0.014\kappa_\infty$ and $\kappa_1 = 0.078\kappa_\infty$. See Sec. V for a discussion of the values of these parameters.

Then, as shown in Fig. 1, the specific heat at constant pressure c_P and the thermal conductivity κ diverge when the critical temperature is approached along the critical isobar. The divergence of c_P is stronger than the divergence of κ.

B. Behavior of the temperature gradient

The unidimensional energy equation at constant pressure reduces to

$$\frac{\partial T}{\partial t} + v\frac{\partial T}{\partial r} = \frac{\chi}{r^g}\frac{\partial}{\partial r}\left(r^g\frac{\partial T}{\partial r}\right) + \frac{1}{\rho c_P}\frac{\partial \kappa}{\partial T}\left(\frac{\partial T}{\partial r}\right)^2, \tag{8}$$

where r is the relevant spatial coordinate, v is the fluid velocity component along r, and g is a number which depends on the geometry:

$$\begin{aligned} &\text{planar symmetry:} \quad g=0,\\ &\text{cylindrical symmetry:} \quad g=1,\\ &\text{spherical symmetry:} \quad g=2. \end{aligned} \tag{9}$$

From Eq. (7), near the CP the dominant part of the derivative of the thermal conductivity is given by

$$\frac{\partial \kappa}{\partial T} \simeq -\,\mathrm{sgn}(T-T_c)\rho_c\frac{\chi_0 c_0}{T_c}\frac{\gamma-\nu}{\beta\delta}\left|\frac{T-T_c}{T_c}\right|^{-(\gamma-\nu)/\beta\delta-1}. \tag{10}$$

Therefore, for the coefficient of the last term on the right-hand side of Eq. (8), we find

$$\frac{1}{\rho c_P}\frac{\partial \kappa}{\partial T} \simeq -\,\mathrm{sgn}(T-T_c)\frac{\chi_0}{T_c}\frac{\gamma-\nu}{\beta\delta}\left|\frac{T-T_c}{T_c}\right|^{-(1-\nu/\beta\delta)}, \tag{11}$$

which corresponds to a quite strong divergent behavior. On the other hand, from Eq. (6) the thermal diffusivity vanishes as ξ^{-1}. A comparison between these two coefficients is shown in Fig. 1, see also Fig. 3 discussed later. Then, near the CP the second term on the right-hand side of Eq. (8) dominates and the energy equation can be approximated by

$$\frac{\partial T}{\partial t} + v\frac{\partial T}{\partial r} = -\,\mathrm{sgn}(T-T_c)\frac{\chi_0}{T_c}\frac{\gamma-\nu}{\beta\delta}\left|\frac{T-T_c}{T_c}\right|^{-(1-\nu/\beta\delta)}\left(\frac{\partial T}{\partial r}\right)^2. \tag{12}$$

Therefore, in order to achieve a balance between convection and diffusion in Eqs. (8), (12), as the temperature approaches the critical value in the hot gaslike side, the spatial derivative of the temperature must vanish according to the power law

$$\frac{\partial T}{\partial r} \propto \left|\frac{T-T_c}{T_c}\right|^{1-\nu/\beta\delta} \tag{13}$$

and consequently the heat flux must vanish following the power law

$$\kappa\frac{\partial T}{\partial r} \propto \left|\frac{T-T_c}{T_c}\right|^{1/\delta}, \tag{14}$$

where use has been made of Eq. (7) together with Eq. (13) and Rushbrooke's and Griffith's scaling laws [18] (see below).

Then, as a consequence of the powerlike divergency of the thermal conductivity with the temperature, when the vaporization takes place along the critical isobar, the heat diffuses only down to a definite locus $R(t)$ defined as the place where

$$T = T_c \quad \text{and} \quad \kappa\frac{\partial T}{\partial r} = 0 \quad \text{at } R(t). \tag{15}$$

On this locus the temperature reaches the critical value and the thermal flow vanishes. Moreover, on the other side of this locus the temperature remains at the initial critical temperature. The heating of the cold fluid takes place as $R(t)$ recedes. The receding velocity, obtained as part of the solution, determines the vaporization time. The vanishing of the heat flux at a moving location is a well known behavior for a thermal diffusivity with a powerlike (although not necessarily diverging) temperature dependence (see, for instance, [21]).

Once this is stated, we define this locus $R(t)$ as the interface between the heated and nonheated regions. This choice appears to be the natural extension of the real thermodynamic interface in subcritical conditions as the critical pressure is attained. Consider that the experiment of isobaric vaporization is repeatedly performed with pressures increasingly higher. As the critical pressure is reached, the heat flux at the interface, on the gas phase side $(\kappa\partial T/\partial r)_{R_+}$, which is proportional to the latent heat times the vaporization rate, will decrease tending to zero, owed to the vanishing of the latent heat at the CP. Then, the conditions stated by Eq. (15) are achieved in the limit of vaporization at the critical pressure.

C. Extrapolation of the model to other dimensionalities

The vanishing heat flux at $R(t)$ is reached for any values of the critical exponents whenever two basic conditions are

accomplished. First, a divergent behavior of the thermal conductivity with a critical exponent $(\gamma-\nu)/\beta\delta>0$ is needed. Second, a divergent behavior of $(1/\rho c_P)(\partial\kappa/\partial T)$ with a critical exponent $1-\nu/\beta\delta>0$ is required. These two conditions may be summarized as

$$\nu<\gamma \quad \text{and} \quad \nu<\delta\beta. \tag{16}$$

The exponent values and the space dimensionality (here denoted by D) are related by the scaling laws [18]

$$2\beta+\gamma=2-\alpha \quad \text{(Rushbrooke's law)},$$

$$2\beta\delta-\gamma=2-\alpha \quad \text{(Griffith's law)},$$

$$\gamma=\nu(2-\eta) \quad \text{(Fisher's law)},$$

$$\nu D=2-\alpha \quad \text{(Josephson's law)}.$$

The first condition in Eq. (16) is accomplished as long as $\eta<1$, which is largely fulfilled, whereas the second condition is always fulfilled for $D>2$, and for the exponent values in Table I it will hold for $D>1.208$. Therefore, the conditions indicated by Eq. (16) are accomplished in any real experiment of vaporization at the CP for all the symmetries indicated in Eq. (9) where $D=3$.

D. The use of a mean field theory

In the previous description of the fluid, a mean field theory has been assumed, neglecting the fluctuations in temperature and density. As we know, these fluctuations become very intense near the critical point. Therefore, one may wonder about the validity of this mean field hypothesis. The mean field theory is accurate only away from the CP, when the correlation length is a microscopic scale and the fluctuations of the order parameter are negligible. As the critical point is approached thermally induced fluctuations of the order parameter develop in many different scales rising to the macroscopic scale. Then, the dynamics becomes governed by the interactions between these clusters regardless of their size and leading to the behavior predicted by the renormalization group theory. The mean field theory neglects the onset and interaction of these critical fluctuations and is thus unable to accurately predict the critical exponents of static (thermodynamic potentials) and dynamic (transport coefficients) properties. Nevertheless, transport phenomena near the CP are usually studied by solving hydrodynamic equations (as the equations considered here) supplemented with the actual behavior of the transport properties involved. In fact, macroscopic hydrodynamic equations are very often used to correlate experimental data and thus account for the predictions of the renormalization group (RG) theory [22,23]. Following these trends, the main aim here is to solve the relevant hydrodynamic equations for the mean values of the macroscopic properties, but considering the critical behavior of the transport properties.

Fluctuations about the mean values occur in a length scale given by the correlation length ξ. These fluctuations may be expected to wipe out whenever the average is performed over regions much larger than ξ. In any thermal relaxation process a characteristic heat conduction length arises, given by

$$L_{\mathrm{HC}}\equiv\frac{T}{\partial T/\partial r}, \tag{17}$$

and the process can be assumed to be governed by a macroscopic model whenever

$$\xi\ll L_{\mathrm{HC}}. \tag{18}$$

In the relaxation process considered here the former condition is expected to be accomplished far from the CP. Moreover, as the critical point is approached along the critical isobar L_{HC} diverges proportionally to

$$L_{\mathrm{HC}}\propto\left|\frac{T-T_c}{T_c}\right|^{-1+\nu/\beta\delta} \tag{19}$$

recalling the exponent renormalization rule for the power laws along different paths [20] we find

$$\frac{\xi}{L_{\mathrm{HC}}}\propto\left|\frac{T-T_c}{T_c}\right|^{[\delta(D-2)-2]/\delta D} \quad \text{at } P=P_c, \tag{20}$$

where use has been made of Rushbrooke's law, Griffith's law, and Josephson's law. Then near the CP the former condition stated by Eq. (18) is translated here to

$$\delta>\frac{2}{D-2}. \tag{21}$$

From Table I it may be concluded that this condition is fulfilled for $D=3$ and it can never be fulfilled for $D=2_+$. Taking into account the exponent values in Table I the condition $\xi\ll L_{\mathrm{HC}}$ will hold for $D>2.67$ (for $\delta=3$) and for $D>2.42$ (for $\delta=4.80$). This provides a self-consistency test of the present scheme for $D=3$ but by no means claims that fluctuations are unimportant. What happens is that the importance of fluctuations is restricted to a neighborhood of the critical point. And even though this length diverges the scale of the region where the temperature is close to the critical temperature shows a stronger divergency and mean values can properly be used.

IV. GOVERNING EQUATIONS

A. Quasisteady profiles

As indicated above, the governing equations are the continuity equation and the energy equation which may be written as

$$\frac{\partial\rho}{\partial t}+\frac{1}{r^g}\frac{\partial}{\partial r}(r^g\rho v)=0 \tag{22}$$

and

$$\frac{\partial T}{\partial t}+v\frac{\partial T}{\partial r}=\frac{1}{\rho c_P r^g}\frac{\partial}{\partial r}\left(r^g\kappa\frac{\partial T}{\partial r}\right) \tag{23}$$

together with the fluid equation of state that relates ρ and T at the critical pressure P_c. Defining the following dimensionless quantities:

$$s \equiv \frac{r}{R_{\text{in}}},$$

$$\tau \equiv \varepsilon \frac{\chi_\infty}{R_{\text{in}}^2} t,$$

$$\omega \equiv \nu \frac{R_{\text{in}}}{\chi_\infty},$$

$$\theta \equiv \frac{T - T_c}{T_\infty - T_c}, \tag{24}$$

$$\varrho \equiv \frac{\rho}{\rho_\infty},$$

$$C \equiv \frac{c_P}{c_{P_\infty}},$$

$$\Lambda \equiv \frac{\kappa}{\kappa_\infty},$$

where $\varepsilon = \rho_\infty / \rho_c$ and $\chi_\infty = \kappa_\infty / \rho_\infty c_{P_\infty}$, the Strouhal and Péclet numbers become

$$\text{St} \equiv \frac{t_{\text{characteristic}}}{t_{\text{residence}}} = \frac{1}{\varepsilon}, \tag{25}$$

$$Pe \equiv \frac{t_{\text{diffusion}}}{t_{\text{residence}}} = 1. \tag{26}$$

Using a reference system which moves with the dimensionless interface $a(\tau) \equiv R(t)/R_{\text{in}}$, we define

$$x \equiv s - a(\tau),$$

$$u \equiv \omega - \varepsilon \dot{a}, \tag{27}$$

$$\dot{a} \equiv \frac{da}{d\tau}.$$

Equations (22) and (23) become, respectively,

$$\varepsilon \left(\frac{\partial \varrho}{\partial \tau} + \frac{g \dot{a} \varrho}{x + a} \right) + \frac{1}{(x+a)^g} \frac{\partial}{\partial x} [(x+a)^g \varrho u] = 0, \tag{28}$$

$$\varepsilon \frac{\partial \theta}{\partial \tau} + u \frac{\partial \theta}{\partial x} = \frac{1}{(x+a)^g \varrho C} \frac{\partial}{\partial x} \left((x+a)^g \Lambda \frac{\partial \theta}{\partial x} \right). \tag{29}$$

Assuming $\varepsilon \ll 1$, a regular expansion of the solutions using ε as a smallness parameter will be performed. To leading order in this regular expansion the unsteady terms in Eq. (28) and Eq. (29) are negligible. Therefore, the QS approximation may be used as the leading order solution.

On the other hand, the fluid on the cold side of the receding border is at rest and at critical conditions. Therefore, in the moving reference system, the boundary conditions at the heated side are

$$\varrho = \frac{1}{\varepsilon} \text{ and } u = -\varepsilon \dot{a} \text{ then } \varrho u = -\dot{a} \text{ at } x = 0. \tag{30}$$

To leading order a first integration of Eq. (28) yields

$$(x+a)^g \varrho u = -a^g \dot{a} \equiv \varphi(\tau), \tag{31}$$

where boundary condition (30) has been used to relate the integration function $\varphi(\tau)$ to the recession velocity $\dot{a}$.

Also to leading order, using θ as the independent variable in Eq. (29), a first integration leads to

$$\varphi(\tau) \int_0^\theta C(\theta') d\theta' = (x+a)^g \Lambda \frac{\partial \theta}{\partial x}, \tag{32}$$

where Eq. (31) and boundary condition (15) have been taken into account.

Separating the x and θ dependent terms in Eq. (32) and integrating, one finds

$$\varphi(\tau) \int_0^x \frac{dx}{(x+a)^g} = \int_0^\theta \frac{\Lambda(\theta'') d\theta''}{\int_0^{\theta''} C(\theta') d\theta'} \equiv F(\theta). \tag{33}$$

Therefore, depending on the geometry considered (i.e., the value of g) the temperature profile will be given by

$$\text{planar:} \quad \theta = F^{-1}(\varphi(\tau) x),$$

$$\text{cylindrical:} \quad \theta = F^{-1}\left[\varphi(\tau) \ln\left(1 + \frac{x}{a} \right) \right], \tag{34}$$

$$\text{spherical:} \quad \theta = F^{-1}\left[\frac{\varphi(\tau)}{a} \left(1 - \frac{a}{x+a} \right) \right].$$

In the cases of planar symmetry or cylindrical symmetry the present solution is not compatible with a constant temperature solution at infinity. Hence, if the heating takes place in contact with an unconfined constant temperature environment, this solution should be matched with an outer solution, thus providing the vaporization rate $\dot{a}$. These cases will not be considered any further here.

On the other hand, in the case of spherical symmetry, the receding velocity is found by imposing the far-field temperature condition, $\theta(x \to \infty) \to 1$, resulting in

$$\frac{\varphi(\tau)}{a} = \int_0^1 \frac{\Lambda(\theta'') d\theta''}{\int_0^{\theta''} C(\theta') d\theta'} = F(1). \tag{35}$$

Using Eq. (31) in Eq. (35) and integrating with respect to time, a d^2 law is obtained,

$$a^2 = 1 - K_{\text{vap}} \tau, \tag{36}$$

with a dimensionless vaporization constant given by

$$K_{\mathrm{vap}}=2F(1). \tag{37}$$

B. Vaporization time

Substituting the value $a=0$ in Eq. (36) one finds the dimensionless vaporization time

$$\tau_{\mathrm{vap}}=\frac{1}{K_{\mathrm{vap}}}. \tag{38}$$

Recalling Eqs. (31), (33), and (37), the vaporization constant—and therefore the vaporization time—may be numerically calculated once the temperature dependence of the variable properties κ and c_P are known—analytically, numerically, or experimentally—in the temperature interval of interest.

Returning to dimensional quantities, the droplet vaporization time is

$$t_{\mathrm{vap}}=\frac{\rho_c}{\rho_\infty}\frac{R_{\mathrm{in}}^2}{\chi_\infty}\tau_{\mathrm{vap}}=\frac{\rho_c R_{\mathrm{in}}^2}{2\int_{T_c}^{T_\infty}\kappa(T'')dT''\Big/\int_{T_c}^{T''}c_P(T')dT'}. \tag{39}$$

It is worth remarking that the integral appearing in Eq. (39) is convergent, in spite of the singular behavior of both κ and c_P near T_c. Recalling Eq. (7), close to the lower integration limit the integrand will behave as

$$\frac{\kappa}{\int_{T_c}^{T}c_P(T')dT'}\sim\left(\frac{T-T_c}{T_c}\right)^{\nu/\beta\delta-1} \tag{40}$$

then the integral will be convergent as long as

$$\frac{\nu}{\beta\delta}>0, \tag{41}$$

which is always true. In any case, for the sake of numerical convergence, the integrations are better performed in terms of the reduced volume $V=\rho_c/\rho$ instead of the temperature. In that case, the vanishing behavior of $(\partial\theta/\partial V)_p$ at the CP compensates the divergency of the specific heat and also that of $\Lambda(\theta)/\int_0^\theta C(\theta')d\theta'$ as $\theta\to 0$.

On the other hand, if the critical behavior is not retained and constant properties are considered, the vaporization time exhibits the logarithmic divergency predicted by the classical theory. If c_P is assumed to be constant and κ variable as was done by Sánchez-Tarifa *et al.* [14] in their model applicable in supercritical conditions, the classical divergency may be cured.

C. Limits of validity of the long-time isobaric scheme

1. Quasisteady approximation

The quasisteady approximation in the reference system receding with the interface defined in Eq. (15) is valid when $\mathrm{St}=1/\varepsilon\gg 1$, which imposes the restriction $\varepsilon\equiv\rho_\infty/\rho_{\mathrm{in}}\ll 1$. That is always true for subcritical vaporization far from the critical point. At the critical pressure the former condition implies the restriction $T_\infty\gg T_c$. If the density at infinity can be evaluated by means of the ideal gas EOS the last restriction may be written as

$$\Theta_\infty\equiv\frac{T_\infty}{T_c}=\frac{Z_c}{\varepsilon}\gg 1, \tag{42}$$

where Z_c is the critical isothermal compressibility

$$Z_c=\frac{P_c}{\mathcal{R}_m T_c\rho_c}\ \text{ with }\ \mathcal{R}_m=\frac{\mathcal{R}_{\text{ideal gas}}}{M_{\text{molar}}}. \tag{43}$$

Here $\mathcal{R}_{\text{ideal gas}}$ is the universal gas constant, and M_{molar} is the molar mass. Experimentally Z_c ranges between 0.23 and 0.31 for most fluids [24], and is equal to 0.375 for a van der Waals gas.

If the smallness parameter is fixed to the acceptable value of 0.05, the estimations of the minimum ambient temperature ($T_{\infty_{\min}}$) for this model to apply are shown in Table II for several fluids of interest in combustion practice.

TABLE II. Minimum ambient temperatures imposed by the long-time condition for various substances, leading to $\varepsilon=0.05$.

Substance	T_c (K)	Z_c	$T_{\infty_{\min}}$ (K)
Hydrocarbons	200–400	0.3	1200–2400
Hydrogen	33.2	0.305	202.5
Nitrogen	126.2	0.29	732
Oxygen	154.6	0.288	890.5
Water	647.3	0.229	2965

Then we see from the values in Table II that condition (42) may be quite restrictive in some cases. Nevertheless it is accomplished in many practical situations, especially for combustion processes when the temperature at infinity corresponds to the adiabatic flame temperature of a diffusion flame located far from the cold fluid package.

2. Isobaric approximation

As reported by [25–31] when the heating takes place in a prescribed volume the piston effect (adiabatic heating), consequence of the thermal expansion coefficient critical divergency, is responsible for the enhanced heating of the fluid. On the other hand, if the heating occurs in an unconfined environment, as it happens in many practical situations, for times much longer than the acoustic time the pressure variations induced by the Stefan flow have a negligible contribution to the heating dynamics. In this situation an isobaric model holds as in the case of unconfined subcritical vaporization.

Now the limits of validity of the former hypothesis are calculated. The pressure variations induced by the Stefan flow may be evaluated by means of the Euler equation,

$$\rho\frac{\partial v}{\partial t}+\rho v\frac{\partial v}{\partial r}=-\frac{\partial P}{\partial r}. \tag{44}$$

In terms of the dimensionless variables defined in Eqs. (24) and (27) together with the definitions

$$\Pi \equiv \frac{P}{P_c}, \tag{45}$$

$$M \equiv \frac{\chi_\infty}{R_{\rm in}}\sqrt{\frac{\rho_\infty}{P_c}}, \tag{46}$$

where Π is the reduced pressure and M is the Mach number, the Euler equation in the moving reference frame reads as

$$\varepsilon\varrho\left(\frac{\partial u}{\partial \tau}+\varepsilon\ddot{a}\right)+\varrho u\frac{\partial u}{\partial x}=-\frac{1}{M^2}\frac{\partial \Pi}{\partial x}. \tag{47}$$

The relative importance of the pressure gradient is given by the squared Mach number

$$\frac{\partial \Pi}{\partial x}=O(M^2). \tag{48}$$

In order to compare the terms corresponding to pressure and temperature inhomogeneities, the energy equation containing the pressure-variation-related terms is rewritten. Making use of the thermodynamic relations

$$\alpha_P \equiv \frac{-1}{\rho}\left(\frac{\partial \rho}{\partial T}\right)_P,$$

$$c_P = c_v + \frac{T\alpha_P}{\rho}\left(\frac{\partial P}{\partial T}\right)_\rho, \tag{49}$$

$$\gamma_a \equiv \frac{c_P}{c_v},$$

where c_v is the mass specific heat at constant volume, the energy equation is written as

$$\varepsilon\frac{\partial \theta}{\partial \tau}+u\frac{\partial \theta}{\partial x}-S\left(\varepsilon\frac{\partial \Pi}{\partial \tau}+u\frac{\partial \Pi}{\partial x}\right) = \frac{1}{\varrho C(x+a)^g}\frac{\partial}{\partial x}\left((x+a)^g\Lambda\frac{\partial \theta}{\partial x}\right),$$

$$\text{where } S \equiv \left(1-\frac{1}{\gamma_a}\right)\left(\frac{\partial \theta}{\partial \Pi}\right)_\varrho. \tag{50}$$

The behavior of the coefficient S corresponding to the pressure variations defined in Eq. (50) can be qualitatively evaluated by means of the van der Waals EOS.

$$S=\left(1-\frac{1}{\gamma_a}\right)\left(\frac{1}{\varrho}-\frac{\varepsilon}{3}\right),$$

$$S_{\rm CP} \simeq \frac{2}{3}\varepsilon = O(\varepsilon), \tag{51}$$

$$S_\infty \simeq 1-\frac{1}{\gamma_{a_\infty}} = O(1).$$

Near the critical point, S becomes $O(\varepsilon)$ and increases up to a value of order $O(1)$ for the conditions at infinity. Moreover, boundary condition Eq. (31) shows that $u \leqslant |\dot{a}| = O(1)$. Then, the isobaric scheme will be consistent as long as

$$O(M^2) \leqslant O(\varepsilon). \tag{52}$$

In the low density limit corresponding to the conditions at infinity, the kinetic theory of dilute gases provides for the thermal conductivity the relation

$$\kappa_\infty \sim c_{v_\infty} l_\infty \sqrt{\rho_\infty P_c}, \tag{53}$$

where l_∞ stands for the mean free path. This yields for the squared Mach number the value

$$M^2 \sim \frac{l_\infty^2}{\gamma_{a_\infty}^2 R_{\rm in}^2}. \tag{54}$$

Then, recalling Eq. (52), the isobaric hypothesis is a good approximation as long as

$$\frac{l_\infty}{R_{\rm in}} \leqslant \sqrt{\varepsilon}, \tag{55}$$

which is always true for macroscopic droplets vaporizing in nonrarified gases, especially if this long-time behavior is expected to be seen, because the characteristic length $R_{\rm in}$ must be large enough for the heating body (the vaporizing droplet in most cases) to last during the first unsteady short-time interval, not considered here, after which the QS temperature profile (34) is reached.

V. VAPORIZATION TIME FOR A VAN DER WAALS DROPLET AT CRITICAL CONDITIONS

The qualitative behavior of the vaporization rate may be analytically worked out in the case of the van der Waals gas, for which

$$P=\frac{\mathcal{R}_m T\rho}{1-b_m\rho}-a_m\rho^2, \quad \text{with } a_m=\frac{27}{64}\frac{\mathcal{R}_m^2 T_c^2}{P_c},$$

$$b_m=\frac{1}{8}\frac{\mathcal{R}_m T_c}{P_c} \tag{56}$$

although the critical exponents predicted by this equation (which corresponds to a mean field theory), differ slightly from the actual exponents provided in Table I.

For a van der Waals gas, the following relations apply:

$$c_v = c_v^{\text{ideal gas}}$$

$$c_P = c_v + \mathcal{R}_m\frac{P+a_m\rho^2}{P-a_m\rho^2(1-2b_m\rho)}. \tag{57}$$

In the framework of a mean field theory the behavior of c_v is nondivergent. In order to find an explicit analytic expression for the vaporization rate an averaged specific heat at constant volume will be considered , $\langle c_v \rangle$, thus the attention will focus on the strong convection due to the thermal expansion, the vanishing of the thermal diffusivity, and the divergency of the thermal conductivity.

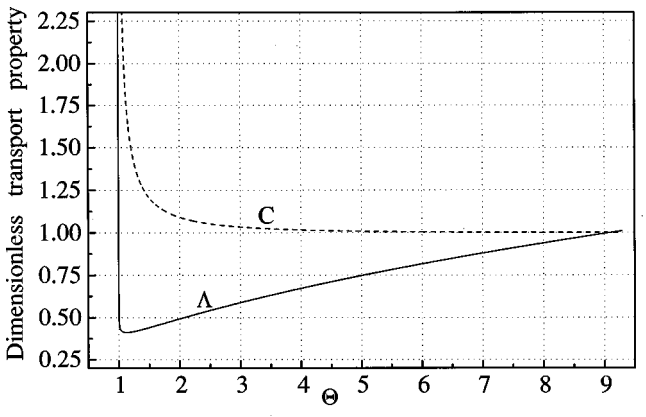

FIG. 2. Temperature dependence of the dimensionless thermal conductivity Λ (solid line) and the dimensionless specific heat C (dashed line) for a van der Waals fluid. Same parameters as in Fig. 1.

An appropriate expression of κ valid for the whole temperature range can be obtained by adding three different contributions [32,22,23]: the low density limit κ^{gas}, the excess thermal conductivity κ^{E}, and the critical divergency at the CP κ^{C},

$$\kappa=\kappa^{\mathrm{gas}}(T)+\kappa^{E}(\rho)+\kappa^{C}(T). \tag{58}$$

For the low density limit two models are considered here, first as assumed by [14] a linear dependence is supposed,

$$\kappa^{\mathrm{gas}}(T)=\kappa^{\mathrm{lin}}\equiv\kappa_{\infty}\frac{T}{T_{\infty}}. \tag{59}$$

Alternatively, the prediction of the kinetic theory for the hard sphere gas is considered,

$$\kappa^{\mathrm{gas}}(T)=\kappa^{\mathrm{HS}}\equiv\kappa_{\infty}\sqrt{\frac{T}{T_{\infty}}}. \tag{60}$$

On the other hand, the excess thermal conductivity is supposed to vary linearly with the fluid density [23]

$$\kappa^{E}(\rho)=\kappa_{1}\frac{\rho}{\rho_{c}} \tag{61}$$

and the critical exponent compatible with the mean field theory is considered (Table I),

$$\kappa^{C}(T)=\kappa_{0}\left|\frac{T-T_{c}}{T_{c}}\right|^{-1/3}. \tag{62}$$

This description of the thermal conductivity is used here just for illustration purposes and will lead to three different contributions to the vaporization constant. Anyway, for any real gas the vaporization rate provided by Eq. (37) may be numerically evaluated taking into account the actual thermodynamic behavior.

In order to visualize the qualitative dependence with the temperature, the thermal conductivity and the specific heat considered here are plotted in Fig. 2 in the case of (as in Fig. 1) a monatomic ($\langle c_v\rangle=\frac{3}{2}\mathcal{R}_m$) hard sphere ($\kappa^{\mathrm{gas}}=\kappa^{\mathrm{HS}}$) gas, with $T_{\infty}=9.3T_c$ (that yields the value $\varepsilon=1/25$), $\kappa_0=0.014\kappa_{\infty}$, and $\kappa_1=0.078\kappa_{\infty}$. To the best of our knowledge, no measurements of the amplitude κ_0 along the critical isobar are available in the literature. For this qualitative calculation the amplitude along the critical isocore for CO_2 [32] has been used. The value of κ_1 corresponds also to CO_2 [32]. In the estimation of both κ_0/κ_{∞} and κ_1/κ_{∞} the approximate value of $\kappa_{\infty}=0.2$ W/mK has been assumed. Figure 2 shows that the critical behavior of the thermal conductivity is important only very close to the critical temperature ($|T-T_c|\simeq 10^{-3}T_c$), whereas the critical enhancement of the specific heat is important even for temperatures as big as $1.25T_c$.

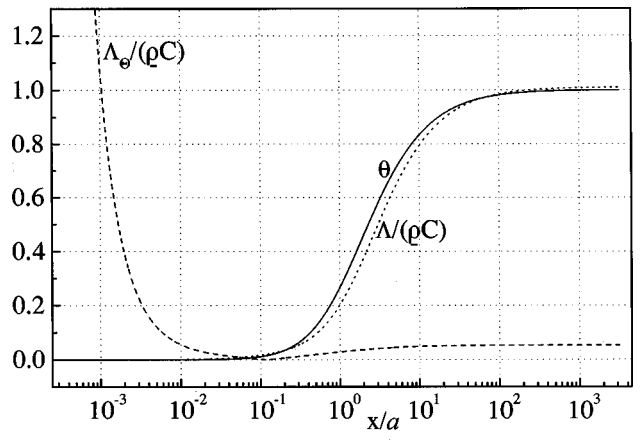

FIG. 3. Linear-log plot of the QS spherically symmetric profiles of the dimensionless thermal diffusivity $\Lambda/\varrho C$ (dotted line), the coefficient $\Lambda_{\Theta}/\varrho C\equiv(1/\varrho C)|\partial\Lambda/\partial\Theta|$ (dashed line), and the receding temperature profile $\theta\equiv(T-T_c)/(T_{\infty}-T_c)$ (solid line) versus the instantaneous distance to the droplet interface x/a for a van der Waals fluid. Same parameters as in Fig. 1.

In Fig. 3 the radial dependence of the dimensionless thermal diffusivity $\Lambda/\varrho C$, the dimensionless coefficient $\Lambda_{\Theta}/\varrho C\equiv(1/\varrho C)|\partial\Lambda/\partial\Theta|$, are shown together with the spherically symmetric QS temperature profile. The three quantities have been calculated from Eqs. (33) and (35) by means of the former model for κ and the van der Waals EOS with the same values of the parameters as discussed before. As mentioned in Sec. II at the droplet (as the critical temperature is approached), the thermal diffusivity vanishes and the divergency of $\Lambda_{\Theta}/\varrho C$ dominates and is responsible for the vanishing thermal flow at the interface. In this plot it is also observed that the critical droplet causes a nonnegligible thermal disturbance in the surrounding atmosphere where it is set even at distances as large as $r\simeq 10^2R_{\mathrm{in}}$.

(a) Gas contribution to the vaporization rate. Recalling Eqs. (33) and (37) the contributions of the terms $\kappa^{\mathrm{gas}}=\kappa^{\mathrm{lin}}$ or $\kappa^{\mathrm{gas}}=\kappa^{\mathrm{HS}}$ to the vaporization rate are found. To leading order in ε the results are, respectively,

$$K_{\mathrm{vap}}^{\mathrm{lin}}=\frac{2c_{P_{\infty}}}{\mathcal{R}_m+\langle c_v\rangle}, \tag{63}$$

$$K_{\mathrm{vap}}^{\mathrm{HS}}=\frac{4c_{P_{\infty}}}{\langle c_v\rangle}. \tag{64}$$

In order to attain a final numerical value of each estimation of K_{vap}, the simplest case of constant c_v is considered.

In these conditions, for a monatomic gas we have $\langle c_v \rangle = \frac{3}{2}\mathcal{R}_m$, and for a diatomic gas $\langle c_v \rangle = \frac{5}{2}\mathcal{R}_m$. Moreover, at infinity Eq. (57) shows that $c_{P_\infty} = \mathcal{R}_m + c_{v_\infty} + O(\varepsilon)$, leading to

$$K_{\text{vap}}^{\text{linmonat}} = K_{\text{vap}}^{\text{lindiat}} = 2, \tag{65}$$

$$K_{\text{vap}}^{\text{HSmonat}} = \frac{20}{3}, \quad K_{\text{vap}}^{\text{HSdiat}} = \frac{28}{5}. \tag{66}$$

Surprisingly enough, the result obtained by means of the van der Waals EOS, considering variable properties and the *mean field* approximate critical behavior of κ and c_P, for the case of $\kappa^{\text{gas}} = \kappa^{\text{lin}}$ coincides exactly with the prediction of Sánchez-Tarifa *et al.* [14], in their model applicable in supercritical conditions where the apparently very restrictive hypothesis of ideal gas EOS, constant c_P, and no singular critical behavior (as it corresponds to supercritical conditions) were taken into account.

(b) Excess contribution to the vaporization rate. The vaporization rate enhancement owed to the excess thermal conductivity is, to leading order in ε,

$$K_{\text{vap}}^{E} = \frac{\kappa_1}{\kappa_\infty}\frac{c_{P_\infty}}{\langle c_v \rangle}\left(\frac{(25c-18)(\pi - 2\arctan 5/\sqrt{16c-9})}{c\sqrt{16c-9}} + \frac{3(c-2)\ln(1+c)/4}{c} - 4 \right), \tag{67}$$

where lower case c is defined as $c \equiv \langle c_v \rangle / \mathcal{R}_m$.

For a constant c_v monatomic or diatomic gas one finds

$$K_{\text{vap}}^{\text{Emonat}} = 1.49\frac{\kappa_1}{\kappa_\infty}, \quad K_{\text{vap}}^{\text{Ediat}} = 1.80\frac{\kappa_1}{\kappa_\infty}. \tag{68}$$

(c) Critical contribution to the vaporization rate. Substituting Eq. (62) in Eq. (37), the critical contribution to the vaporization rate to leading order in ε is

$$K_{\text{vap}}^{C} = \frac{\kappa_0}{\kappa_\infty}\frac{c_{P_\infty}}{\mathcal{R}_m}\frac{4}{\sqrt[3]{3}}\int_0^\infty \frac{(z+3)/(z+1)^{1/3}}{(1+c)z^2 + 5z + 4}\,dz \tag{69}$$

and for a monatomic or a diatomic constant c_v gas

$$K_{\text{vap}}^{\text{Cmonat}} = 11.20\frac{\kappa_0}{\kappa_\infty}, \quad K_{\text{vap}}^{\text{Cdiat}} = 13.06\frac{\kappa_0}{\kappa_\infty}. \tag{70}$$

(d) Relative decrease of the vaporization time. Separating the integral that defines the vaporization rate according to the expression of κ, K_{vap} is found to be the sum of the three contributions

$$K_{\text{vap}} = K_{\text{vap}}^{\text{gas}} + K_{\text{vap}}^{E} + K_{\text{vap}}^{C}. \tag{71}$$

The dimensionless vaporization time may be calculated by means of Eq. (38) and the relative decrease of the vaporization time owed to a contribution K_{vap}^{j} is given by

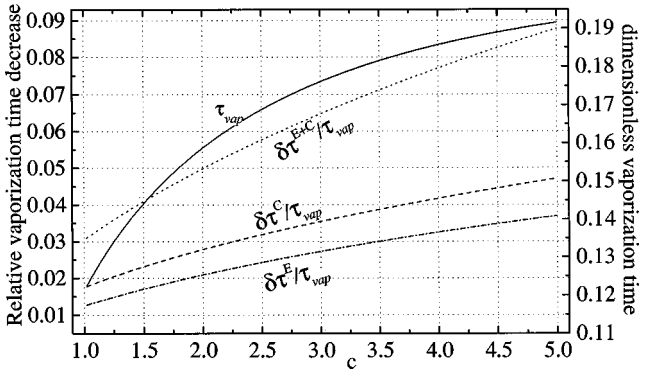

FIG. 4. Relative vaporization time decrease (left axis scale) owed to the excess thermal conductivity (dot-dashed line), the critical thermal conductivity (dashed line), and the combination of both effects (dotted line) together with the dimensionless vaporization time (right axis scale) as a function of $\langle c_v \rangle / \mathcal{R}_m$ for a van der Waals fluid. Same parameters as in Fig. 1.

$$\frac{\delta\tau_{\text{vap}}^{j}}{\tau_{\text{vap}}} = \frac{K_{\text{vap}}^{j}}{\sum_{i \neq j} K_{\text{vap}}^{i}}. \tag{72}$$

The relative decreases of the vaporization time owed to κ^C, κ^E and to the combined effect of both contributions are plotted in Fig. 4 together with the dimensionless vaporization time as a function of the averaged specific heat at constant volume c, see figure caption for details. It may be seen that, with the values of κ_0 and κ_1 used in this calculation, the influence of κ^C is always bigger than that of κ^E. Both contributions to the vaporization rate grow with the averaged specific heat at constant volume c. Thus this decrease in the vaporization time in critical conditions may be quite important for polyatomic molecules.

In the case of constant c_v, for a monatomic or a diatomic gas, the relative decrease owed to the combined effect of κ^C and κ^E for other values of κ_0 and κ_1 is given by

$$\frac{\delta\tau_{\text{vap}}^{\text{monat}}}{\tau_{\text{vap}}^{\text{monat}}} = 0.22\frac{\kappa_1}{\kappa_\infty} + 1.68\frac{\kappa_0}{\kappa_\infty}, \qquad \frac{\delta\tau_{\text{vap}}^{\text{diat}}}{\tau_{\text{vap}}^{\text{diat}}} = 0.32\frac{\kappa_1}{\kappa_\infty} + 2.33\frac{\kappa_0}{\kappa_\infty}. \tag{73}$$

Finally, the vaporization time for a constant c_v, monatomic or diatomic hard sphere gas, for other values of κ_0 and κ_1, is given by

$$t_{\text{vap}}^{\text{monat}} = \frac{\frac{3}{8}\mathcal{R}_m \rho_c R_{\text{in}}^2}{\kappa_\infty + 1.68\kappa_0 + 0.22\kappa_1}, \qquad t_{\text{vap}}^{\text{diat}} = \frac{\frac{5}{8}\mathcal{R}_m \rho_c R_{\text{in}}^2}{\kappa_\infty + 2.33\kappa_0 + 0.32\kappa_1}. \tag{74}$$

VI. CONCLUSIONS

The convective-diffusive heating of a fluid package at critical conditions, immersed in a much hotter environment, has been considered. Due to the diverging behavior of the thermal conductivity the heat flux must vanish at a definite locus $R(t)$ where the critical conditions are reached. This locus separates two distinguishable regions. On one side there is the hot gaslike region and on the other side there is the fluid package at the initial critical conditions. The locus $R(t)$ appears to be the natural extension of the subcritical interface when the critical pressure is approached from below. Thus the position $R(t)$ is defined as the interface for the Stefan problem at critical conditions. The heating of the cold fluid package takes place as the interface recedes with time.

The way to account for a nondiverging vaporization rate at critical conditions, when the latent heat term is absent and there is no density difference across the interface $R(t)$, is to take into account the critical divergency of the specific heat and the thermal conductivity, which causes a vanishing heat flow at the interface.

When the ratio between the gas density and liquid density is small, a regular expansion of the equations using $\varepsilon \equiv \rho_\infty/\rho_c \ll 1$ as the smallness expansion parameter can be performed. Then, the evolution of the system in the long-time limit is quasisteady when seen from a reference frame attached to the receding interface. The receding temperature profiles found in the cases of planar and cylindrical symmetry are not compatible with a constant temperature solution at infinity. In these cases the receding velocity of the interface should be found as a consequence of the matching between the present solution and the far-field solution. In the spherical symmetry case, which is the case of interest in droplet vaporization, the boundary condition of constant temperature at infinity determines the receding velocity of the interface, and a d^2 law with a finite vaporization rate is found. Moreover, the vaporization rate and the vaporization time are given by a quadrature that can be numerically evaluated once the specific heat at constant pressure c_P and the thermal conductivity κ are known in the temperature interval of interest.

Thus, the present model of droplet vaporization permits us to establish a quasisteady scheme, in the moving reference frame, applicable along the critical isobar that, according to the experimental evidence, predicts a minimum, nonvanishing, vaporization time when the pressure is the critical pressure of the droplet, as compared to the vaporization time in subcritical conditions for $P < P_c$. The reason for this minimum, but nonvanishing, vaporization time at critical pressure is twofold. On one hand, the latent heat term is absent and, on the other hand, there is an extra contribution to the vaporization rate owed to the critical behavior of the thermal conductivity.

The hypothesis of small density ratio $\varepsilon \equiv \rho_\infty/\rho_c$ imposes the condition of a very high temperature at infinity; this condition may be quite restrictive in some cases but it is fulfilled in many practical situations, especially for droplet combustion at critical conditions when the vaporizing droplet is surrounded by a far diffusion flame.

The restrictions imposed by the hypothesis of isobaric behavior are analyzed by means of the Euler equation. In the long-time limit considered here it is found that the pressure variations induced by the Stefan flow will be of order $O((l_\infty/R_{\mathrm{in}})^2)$, with l_∞ being the mean free path at infinity and R_{in} the initial droplet radius. Then we conclude that, in the long-time limit, the isobaric hypothesis will be a good approximation for macroscopic droplets vaporizing in unconfined nonrarified media, even if the droplet is at critical conditions.

The model shows that the d^2 law remains valid for droplet vaporization at critical conditions. The droplet vaporization time is given by Eq. (39) and it may be evaluated once the fluid specific heat and the thermal conductivity are known as a function of the temperature in the range of interest.

The qualitative behavior of the vaporization rate and the vaporization time are analytically calculated for a van der Waals EOS, an averaged specific heat at constant volume $\langle c_v \rangle$, and a thermal conductivity compatible with the mean field theory in the critical region and with the kinetic theory in the low density region. In this analysis it is found that the relative vaporization time decrease owed exclusively to the thermal conductivity divergency is close to 7.5%, being more important for polyatomic molecules.

ACKNOWLEDGMENTS

This work has been supported by DGESIC-MEC Spain, under Project Nos. PB94-0385 and PB97-0159, and also by AFOSR Grant No. F49620-97-1-0098, which financed the stay of P.L.G.-Y. at the CECR (University of California, San Diego). The hospitality and advice of Professor Forman A. Williams at CECR is also gratefully acknowledge.

[1] A. Williams, Combust. Flame **21**, 1 (1973).
[2] B. N. Raghunandan and H. S. Mukunda, Combust. Flame **30**, 71 (1977).
[3] W. A. Sirignano, Prog. Energy Combust. Sci. **9**, 291 (1983).
[4] S. D. Givler and J. Abraham, Prog. Energy Combust. Sci. **22**, 1 (1996).
[5] F. A. Williams, *Combustion Theory* (Benjamin/Cummings, Menlo Park, 1985).
[6] A. Crespo and A. Liñán, Combust. Sci. Technol. **11**, 9 (1975).
[7] T. Kadota and H. Hiroyasu, *Eighteenth Symposium (International) on Combustion* (The Combustion Institute, Pittsburgh, 1981), p. 275.
[8] J. Sato, M. Tsue, M. Niwa, and M. Kono, Combust. Flame **82**, 142 (1990).
[9] J. Sato, AIAA Report No. 93-0813, 1993.
[10] B. Vieille, C. Chauveaux, X. Chesneau, A. Odeïde, and I. Gökalp, *Twenty-Sixth Symposium (International) on Combustion* (The Combustion Institute, Pittsburgh, 1996), p. 1259.
[11] H. Nomura, Y. Ujiie, H. J. Rath, J. Sato, and M. Kono, *Twenty-Sixth Symposium (International) on Combustion* (The

Combustion Institute, Pittsburgh, 1996), p. 1267.
[12] D. B. Spalding, ARS J. **29**, 828 (1959).
[13] D. E. Rosner, AeroChem Research Labs, Princeton, NJ Report No. TP-128, 1966.
[14] C. Sánchez-Tarifa, A. Crespo, and E. Fraga, Astron. Acta **17**, 685 (1972).
[15] D. E. Rosner and W. S. Chang, Combust. Sci. Technol. **7**, 145 (1973).
[16] P. Haldenwang, C. Nicoli, and J. Daou, Int. J. Heat Mass Transf. **39**, 3453 (1996).
[17] H. E. Stanley, *Introduction to Phase Transitions and Critical Phenomena* (Oxford University Press, New York, 1971).
[18] J. J. Binney, N. J. Dowrick, A. J. Fisher, and M. E. J. Newman, *The Theory of Critical Phenomena* (Oxford University Press, New York, 1992).
[19] K. Kawasaki, Phys. Rev. **150**, 291 (1966); in *Phase Transitions and Critical Phenomena*, edited by C. Domb and M. S. Green (Academic, New York, 1976), Vol. 5A; Ann. Phys. (N.Y.) **61**, 1 (1970).
[20] J. M. H. Levelt Sengers, in *Supercritical Fluid Technology*, edited by T. J. Bruno and J. F. Ely (CRC Press, Boca Raton, FL, 1991), p. 1.
[21] L. D. Landau and E. M. Lifshitz, *Fluid Mechanics*, 2nd ed. (Pergamon Press, New York, 1987), p. 202.
[22] V. Vesovic and W. A. Wakeham, in *Supercritical Fluid Technology*, edited by T. J. Bruno and J. F. Ely (CRC Press, Boca Raton, FL, 1991), p. 245.
[23] C. A. Nieto de Castro, in *Supercritical Fluid Technology*, edited by T. J. Bruno and J. F. Ely (CRC Press, Boca Raton, FL, 1991), p. 335.
[24] S. I. Sandler, *Chemical Engineering Thermodynamics* (Wiley, New York, 1989).
[25] A. Onuki, H. Hao, and R. A. Ferrell, Phys. Rev. A **41**, 2256 (1990).
[26] H. Boukari, J. N. Shaumeyer, M. E. Briggs, and R. W. Gammon, Phys. Rev. A **41**, 2260 (1990).
[27] B. Zappoli, D. Bailly, Y. Garrabos, B. Le Neindre, P. Guenoun, and D. Beysens, Phys. Rev. A **41**, 2264 (1990).
[28] M. Bonetti, F. Perrot, D. Beysens, and Y. Garrabos, Phys. Rev. E **49**, R4779 (1994).
[29] A. Onuki and R. A. Ferrel, Physica A **164**, 245 (1990).
[30] J. Straub, L. Eicher, and A. Haupt, Phys. Rev. E **51**, 5556 (1995).
[31] J. Straub and L. Eicher, Phys. Rev. Lett. **75**, 1554 (1995).
[32] J. V. Sengers, in *Transport Phenomena*, edited by J. Kestin, AIP Conf. Proc. No. 11 (AIP, New York, 1973), p. 229.